Controlling the Morphology of PEDOT:PSS Blend Films with Pre-Deposition Solution Composition and Deposition Technique

Luke Heroux^{1,2}, Josh Moncada³, Mark Dadmun* ^{3,4}

- 1- University of Tennessee Knoxville, Department of Material Science & Engineering
 - 2- Oak Ridge National Laboratory, Neutron Sciences Division
 - 3 University of Tennessee Knoxville, Department of Chemistry
 - 4 Oak Ridge National Laboratory, Chemical Sciences Division

Abstract

Understanding the relationships between morphology, fabrication processes, and thermoelectric performance in conducting polymers is essential to the development of highefficiency organic thermoelectrics as an alternative to commonly used rare metals. Altering the film fabrication process of Poly(3,4-ethylenedioxythiophene): poly(styrene sulfonate) (PEDOT:PSS) with the addition of high boiling solvents to the precast solution improves the electrical conductivity and significantly increases its Seebeck value. Neutron scattering monitors the changes in the atomic, nanoscale and mesoscale morphology of PEDOT:PSS thin films with the addition of dimethyl sulfoxide (DMSO) to the aqueous solution prior to film formation and with varying fabrication procedures. The neutron scattering results show a decrease in the deuterated PSS (dPSS) domain size along with systematic variations in PEDOT fibril assemblies in the final blend film with the addition of DMSO to the pre-deposition solution. These structural modifications indicate that the reported increase in conductivity of PEDOT:PSS blends with addition of DMSO reported in the literature can be ascribed to the disruption of solvated PEDOT assemblies by the DMSO, forming smaller PSS domains in the predeposition solution, allowing smoother film formation. These improvements are observed significantly with the addition of just 1% DMSO, but continue to modestly improve with the addition of up to 5% DMSO to the PEDOT:PSS blend pre-deposition solution. The fact that the variations in the measured morphology are independent of whether the films were deposited by spin or ultra-sonic spray casting methods emphasizes the crucial importance of the structure of the blend in the pre-deposition solution in determining the final thin film blend morphology.

^{*}Corresponding Author (Dad@utk.edu)

Introduction

Conducting polymers are an important class of materials, where their use in energy harvesting applications aid in the development of technologies to improve sustainability. Thermoelectric materials transform a temperature gradient to an electric current, or inversely an electric potential to a change in temperature. Thermoelectrics have been useful in commercially available energy technologies; for instance, they are commonly found in photovoltaics for solar-energy generation and light-emitting diodes. 1,2,31 The efficiency of a material in converting a thermal gradient to an electric potential is given by the dimensionless figure of merit ZT, which is calculated by $ZT = \frac{S^2 \sigma T}{\kappa}$. In this equation, S is the Seebeck coefficient of the material, σ its electric conductivity, T is the temperature, and κ is its thermal conductivity. Most common thermoelectrics with high ZT's are inorganic materials consisting of rare metals, for instance BiSbTe or Bi2Te3/Sb2Te3 super lattice domains exhibit ZT=1.2 and 2.4, respectively.^{4,5} However, these inorganic materials are brittle, and expensive to obtain and fabricate thermoelectrics from. On the other hand, thermoelectric polymers offer a flexible material that can conformally coat an object and offer ease of processing that is scalable for commercial manufacturing of high-quality films. 6 Thus, these organic thermoelectrics provide an inexpensive and viable alternative to the brittle rare metals that are currently more common in thermoelectric applications. However, the performance of organic thermoelectrics lags that of inorganic thermoelectrics. Thus, a more thorough understanding of how the thermoelectric performance of these promising materials can be tuned is needed. For instance, previous studies have shown that alteration of the film formation conditions result in a dramatic improvement in thermoelectric performance. Thus, understanding the relationships between

fabrication processes, morphology development during fabrication, and thermoelectric performance in conducting polymer constructs is needed to move this field towards the rational development of organic thermoelectrics with optimal performance.

Poly(3,4-ethylenedioxythiophene):poly(styrene sulfonate) (PEDOT: PSS) is a promising and commonly studied conjugated polymer blend that currently has the highest reported ZT (0.25 with no doping, and 0.42 with DMSO doping) of any organic material at room temperature.^{7,8} Moreover, previous studies have shown that altering the film fabrication process such as including the addition of high boiling solvents to its precast solution or immersion of the cast film in ethylene glycol dramatically impacts its electrical conductivity and Seebeck value.⁸⁻¹⁶²² More precisely, the addition of dimethyl sulfoxide (DMSO) to the predeposition PSS:PEDOT solution has been shown to increase the electrical conductivity and lower the Seebeck coefficient of a film that is formed from that solution. 9 Some of these studies have shown an increase in electrical conductivity by as much as a factor of 1000. 109,10 For instance, Dimitriev, et al, reported that the conductivity increased by a factor of 4 with the addition of just 1% DMSO and an order of magnitude increase with the addition of 5% DMSO to the pre-deposition solution. Further studies using small and ultra-small angle neutron scattering showed that adding DMSO to the pre-deposition solution altered the morphology of spray coated films. 10,11 In these studies, it was observed that the local fibril-like PEDOT domains decrease in size and become more uniformly shaped with addition of DMSO. This improved uniformity of PEDOT fibrils in the larger PSS domain resulted in enhanced conductivity due to better mesoscale ordering, with increases in conductivity by a factor of 800.¹⁰

Additional studies, using techniques such as atomic force microscopy (AFM), scanning electron microscopy (SEM), and Raman Spectroscopy have provided insight into how altering the film fabrication technique improves the conductivity of the thermoelectric film. Varying the film coating technique alters the smoothness and wetting, which are monitored by imaging the film surface. ^{6,11,12} Particularly, the thickness, wetting, and roughness of the deposited films varied with the surface tension, contact angle, viscosity, and deposited drop sizes in spray coated films, which varied with pre-deposition concentrations of DMSO. 6,11,12 Zabihi, et al., observed that the spin coating created a stratified structure with an upper PSS-rich layer on a PEDOT-rich lower layer. The structure and surface roughness of the upper PSS-rich layer varies with substrate temperature and annealing temperature, which impacts film conductivity. 12 Smoother surfaces, especially surfaces which displayed fewer large domains as observed in AFM and SEM, were the most conductive. ¹² These studies also verify that the PEDOT: PSS films are smoother at the meso-scale length scale and exhibit higher conductivity when spin-coated than when spray coated. These reports also showed that spin cast surfaces tend to be smoother with the addition of DMSO to the pre-deposition solution than without, leading to further increases in conductivity. 12 Additionally, Ouyang et al, observed that the increase in conductivity occurs only when additives are included in the liquid pre-deposition solution and are then annealed. 6,14

To date, few studies have been performed to clearly identify the morphology of PEDOT:PSS blend films and correlate its structure to its performance as an organic thermoelectric. The studies that have been published use various compositions of PEDOT:PSS solutions and additives with different treatments and coating methods.⁸⁻¹² The existing

knowledge of morphological changes is often limited to the length scale of the techniques used, whether that be AFM, Raman Spectroscopy or neutron scattering. 9,11,12,14 Of these investigations, only a couple have addressed the changes in morphology over a broad range of length scales. 9,11 Additional studies suggest that the morphology of the PEDOT:PSS system undergoes observable changes across a broad range of length scales, from atomic- to nano- to micron length scales, with incremental variation in pre-deposition solution composition. 12-14 Therefore, analysis of the structure over the aforementioned length scales offers crucial insight into how the morphology of the blend and ordering of its components varies with film formation conditions. In this study, we focus on the variation of the blend film structure with deposition technique (spin coating to spray coating) as well as the loading of DMSO in the predeposition solvent. Using small-angle and ultra-small-angle neutron scattering provides insight into the morphological changes in PEDOT:dPSS films on length scales that range from 10's of angstroms up to 100's of microns. 17

Specifically, we have explored how the morphology of the Poly(3,4-ethylenedioxythiophene): deuterated poly(styrene sulfonate) (PEDOT:dPSS) polymer blend varies when cast by spin coating or spray coating, coupled to the impact of the presence of DMSO in the pre-deposition solution on the structure of the deposited film. We monitored the change in PEDOT:dPSS structure when 1% wt., 3% wt. and 5% wt. DMSO was added to the pre-deposition solution and compared the structure of these as-cast films using small-angle neutron scattering. These results provide insight into the relative importance of deposition technique and predeposition solution structure on final film morphology and provide insight that can be used to optimize the performance of PEDOT:PSS blend films in functional applications.

Experimental Methods

Synthesis

PEDOT:dPSS (1.3%wt.) in aqueous solutions were created by the polymerization of 3,4-ethylenedioxythiophene (EDOT) in a deuterated poly(styrene sulfonate) (dPSS) aqueous solution following the BAYTRON P synthesis as described in the literature. ¹⁹⁻²² In this polymerization, EDOT monomers from TCI America were oxidatively polymerized in an aqueous dPSS (Mw 429 kDa, PDI 1.15, Polymer Source Inc. Canada) solution using charge balancing counter ions Na₂S₂O₈ (Sigma-Aldrich, USA) and Fe₂(SO₄)₃·5H₂O (Acros-Organics, USA). This bulk solution was separated into smaller volumes to create a series of solutions with a range of DMSO loadings. To remove large aggregates that may have formed, the blend solutions were then filtered 3 times through 5-micron syringe filters.

Film Formation

The solutions were deposited to form films by spin coating and spray coating onto Silicon crystal wafer substrates that have been etched with piranha (3:1 sulfuric acid and hydrogen peroxide) and oxidized under ultra-violet light. All cast films were annealed at 413K for 20 minutes to remove any excess water and dopant.

Spin coated films were fabricated using 1ml of solution spun at 1000 rpm for 90 seconds as illustrated in Figure 1. Speed and duration of deposition were chosen based on common parameters used in other studies as well as to optimize consistency of the coating and maintain a conductive surface. The conductivity in all films was confirmed using an ohmmeter.

Spray coated films were deposited using a custom-built jet-nozzle sprayer that transitions across the substrate as illustrated in Figure 1. Nozzle speed was adjusted to a

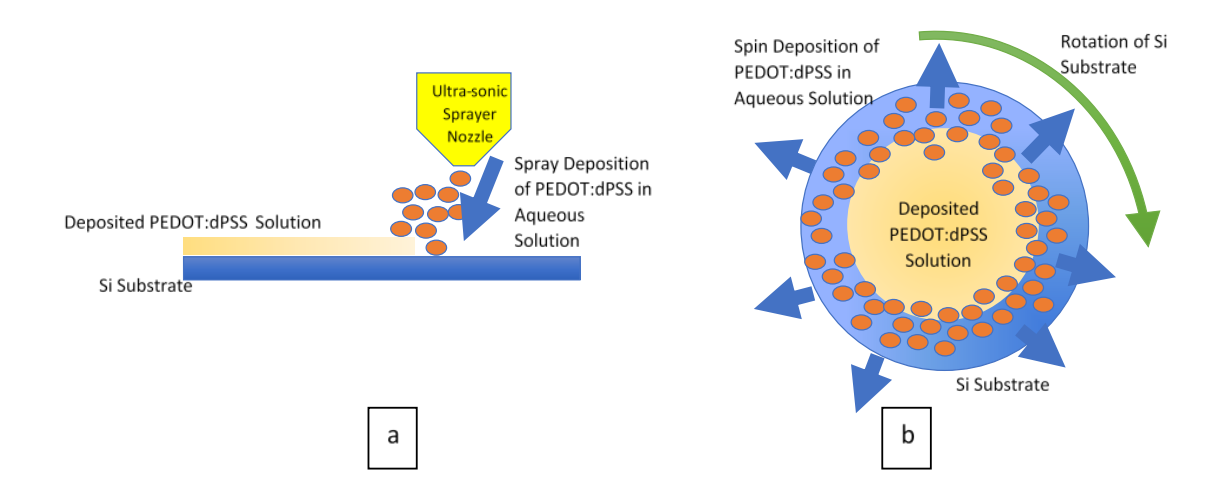


Figure 1 – Illustration of deposition processes that occur during the formation of PEDOT:dPSS films on Si Substrates. Spray coating with use of custom built ultra-sonic nozzle (a) and spin coating (b).

minimum spray speed of around 0.05 ml/sec to achieve a smooth consistent coating that was also conductive. 30 spray passes were made to achieve well distributed visually consistent films.

Neutron Scattering

Substrates with deposited films were physically divided into smaller pieces of 1.2cm squares post-deposition to fit into sample containers on all neutron scattering instruments. ¹⁶ Si wafers with polymer film were stacked to increase scattering statistics, giving a total film thickness in the neutron beam of 50 microns for spray coated samples and 5 microns for spin coated samples. All neutron measurements were taken at room temperature (~298K) and were normalized to transmission as well as for thickness of samples. ²³ Sample container and Si wafer background scattering were subtracted from sample scattering to obtain the scattering of the PEDOT:dPSS films.

To monitor the structure of the PEDOT:dPSS blend films over a broad range of length scales, four neutron scattering instruments were used. At Oak Ridge National Laboratory (ORNL), these were the General Purpose Small Angle Neutron Scattering (GP-SANS) instrument at the High Flux Isotope Reactor with a neutron wavelength (λ) range of λ = 4.75Å, 6 Å, and 18Å; and the Ultra-Small Angle Neutron Scattering (USANS) instrument at the Spallation Neutron Source with distinct wavelengths of λ/n , where $\lambda=3.6\text{Å}$, and the harmonic peak n=1-5.^{17,24} At the National Institute of Standards and Technology (NIST) Center for Neutron Research, the instruments used were the Very Small-Angle Neutron Scattering (VSANS) instrument, measured using two wavelengths of $\lambda=5\text{Å}$ and $\lambda=17\text{Å}$; and the USANS instrument, measured using $\lambda=5\text{Å}.^{25}$ The combinations of these experiments provide data over a merged Q-range, from 1 x 10⁻⁶ A⁻¹ up to 5 x 10⁻¹ A⁻¹, which covers real space length scales that span microns to nanometers using USANS and nanometers to angstroms using the SANS/VSANS instruments and is defined by the scattering vector, Q, in reciprocal space according to Bragg's Law, $Q=rac{4\pi\sin(heta)}{\lambda}$, where λ is the wavelength of the neutrons, and θ is the scattering angle.

Reduction of the raw data from ORNL was performed using Mantid, while reduction of the raw data from NIST was performed using IGOR pro 8.^{26,27} All data were combined and USANS point-space data was scaled to the normalized SANS data.²⁸ The VSANS data overlays the GP-SANS data and was therefore omitted from the final fits but was used to properly scale USANS data. Fitting and analysis were performed using SasView.²⁹ The data were fit to models that included a combination of the Debye-Anderson-Brumberger (DAB) model and the elliptical

Table 1- Correlation length (L), minor (r_{min}) and major (r_{maj}) radii in both spin and spray deposited films.

	Cor length, L (Å)	Minor Radius , r _{min} (Å)	<u>Major Radius, r_{maj}</u> (Å)
Spin Pristine	52776 ± 0.24	90.00 ± 3.4	540 ± 5.14
Spin 1% DMSO	15098 ± 0.26	4.92 ± 4.8	168 ± 2.10
Spin 3% DMSO	11700 ± 0.13	200.00 ± 0.02	10000 ± 8.1
Spin 5% DMSO	7500 ± 0.03	12.00 ± 1.7	12 ± 0.03
Spray Pristine	100000 ± 596	9.00 ± 3.2	810 ± 8.3
Spray 1% DMSO	29117 ± 754	4.46 ± 4.1	3416 ± 6.47
Spray 3% DMSO	22788 ± 459	82.00 ± 1.59	9102 ± 4.89
Spray 5% DMSO	15000 ± 0.03	50.00 ± 0.01	750 ± 0.01

cylinder form factor. 30-33 The DAB model is captured in the first term of Equation 1 below, which

was developed to model, and often used to characterize, the structure of two-phase systems. 10,30,31 The elliptical cylinder form factor is described as the second term in Equation 1 and has been applied to model and characterize the parallelepiped and cylindrical shaped structures in crystalline assemblies. 10,34,35 The DAB equation models the phase separated structure of the polymer blend, thus describing the morphology and size of the two polymer domains, parameterized as the correlation length, L, which is a measure of the average distance between dPSS domains. This structural feature dominates the scattering in the lowest Q region, and thus is primarily measured using USANS. The elliptical cylinder models the average cross-sectional size and shape of the PEDOT fibrillar crystals that form in the phase separated polymer blend. The elliptical cylinder model quantifies the size of the cross section of the PEDOT crystals by providing the minor radius, r_{min} , and ratio of minor and major radii, v, which is then used to calculate the major radius, $r_{maj} = v/r_{min}$, as well as the length of the cylinder, H. These length scales are primarily measured in the mid to high Q regions using SANS.

$$I(q) = A_1 \frac{L^3}{(1 + (q \times L)^2)^2} + A_2 \frac{1}{V_{CVI}} \left(\frac{J(a)\sin(b)}{ab}\right)^2 + background$$
 (1)

In Equation 1, L is the correlation length of the PSS:PEDOT film and the normalization factor, $A_1=8\pi\Phi(1-\Phi)\Delta\rho^2$. Here $\Delta\rho^2$ is the neutron scattering length density contrast of the two phases , and Φ represents the volume fraction of one phase. In the second term, A_2 is a prefactor, V_{cyl} is the volume of the cylinder, and J(a) is the Bessel function, where a and b are the radii defined as, a=Qr', and b=QH, where H is the cylinder length and r'= $r_{\min}\sqrt{2(1+v^2)}$.

Results

The neutron scattering curves of PEDOT:dPSS films that were formed from aqueous solutions containing varying amounts (0% wt., 1% wt., 3% wt., and 5% wt.) of DMSO were measured. The impact of deposition technique was also studied, where both spin-coated and spray coated

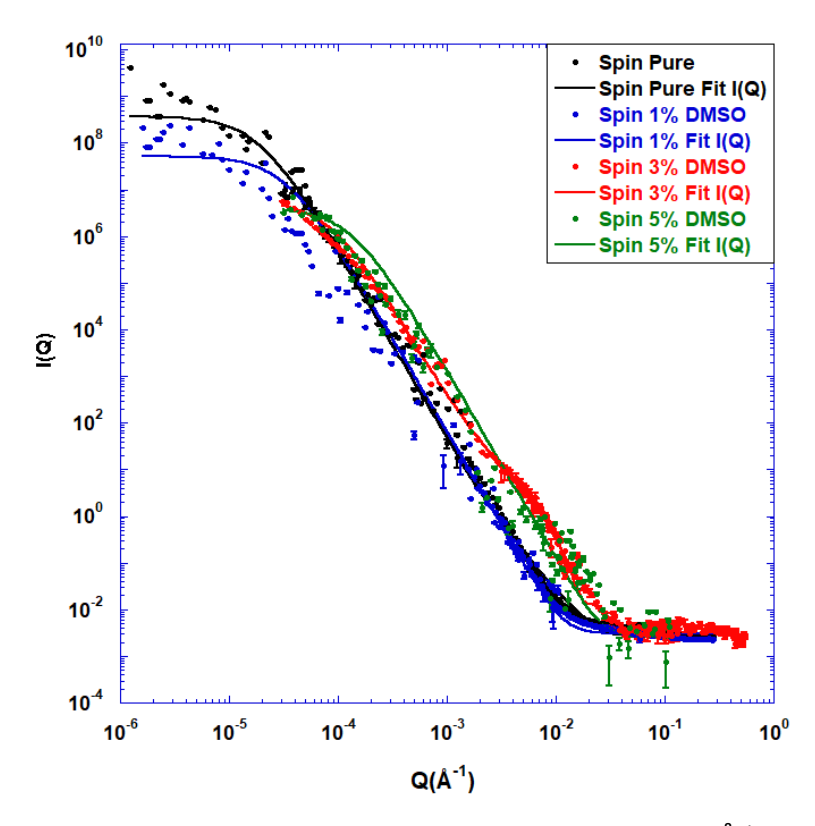


Figure 2 – Plot of neutron scattering intensity (I(Q)) as a function of Q ($Å^{-1}$) for spin coated films. SANS data for Pristine (black), 1%wt DMSO (blue), 3%wt DMSO (red), and 5%wt DMSO (green) solutions are dots and corresponding fits to Equation 1 are lines.

films were examined. These scattering curves are analyzed to determine the impact of these fabrication parameters on the nanoscale and mesoscale structure of the formed polymer blend thin films. These scattering curves and their fits to the DAB-elliptical cylinder model as described in Equation 1 are shown in Figures 2 and 3. The correlation length (L) of the phase separated domains, as well as the minor (r_{min}) , and major radius (r_{maj}) of the PEDOT fibrils are also presented in Table 1 for the samples studied. The fitting of the data to the model was insensitive to the cylindrical length, H, which consistently attained very large values (> 31000 Å).

Impact of addition of DMSO to pre-deposition solution on blend morphology

Inspection of these results shows that as DMSO is added to the solution, the sizes of the dPSS domains in the film dramatically decrease, as quantified by the change in the correlation

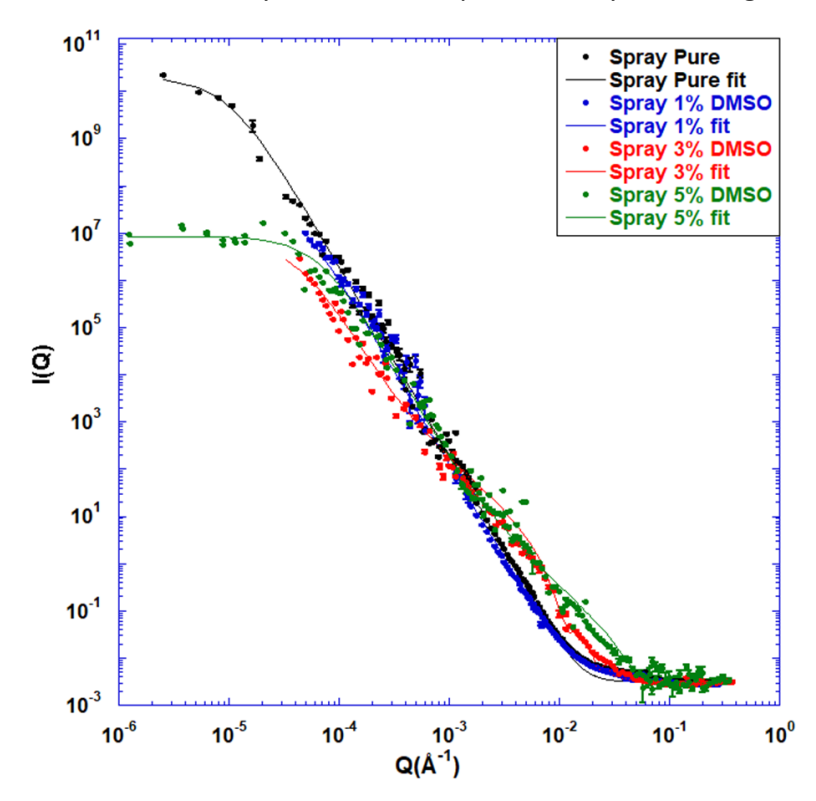


Figure 3 – Plot of neutron scattering intensity (I(Q)) as a function of Q ($Å^{-1}$) for spray coated films. SANS data for Pristine (black), 1%wt DMSO (blue), 3%wt DMSO (red), and 5%wt DMSO (green) solutions are dots and corresponding fits to Equation 1 are lines.

length. The correlation length in the spin coated films decreases from 5.2 microns to about 1.5 microns with the addition of 1% DMSO, a 70% decrease in size. Addition of more DMSO to the pre-deposition solution, 3% and 5% DMSO, further decreases the correlation length to 1.2 microns and 0.75 microns, respectively. These values correspond to a 78% and 85% decrease, respectively, in domain size when compared to the domains formed from pure aqueous solution. This decrease in correlation length establishes the formation of smaller dPSS domains in the spin-cast films with the addition of DMSO to the pre-deposition solution. This is consistent with the formation of smaller dPSS domains in solution with addition of DMSO to the pre-deposition solution, as illustrated in Figure 4a. These results are also consistent with studies that showed smoother surfaces and increases in conductivity in PEDOT:PSS films with addition of DMSO to pre-deposition solutions. 8-10,12

While analysis of the lowest Q region provides information on the micron-scale domain structure (L), analysis of the higher Q regions (smaller length scales) provides information on the smaller PEDOT crystalline fibril structure ($r_{min} \& r_{maj}$). This analysis shows that the PEDOT crystalline fibrils form domains with rectangular or elliptical cross-sections and the size of these fibrils in the film changes with the addition of DMSO to the pre-deposition solution and with the deposition technique. First, the addition of 1% DMSO to the pre-deposition solution decreases both the minor radius and the major radius of the fibril in the film, starting a fluctuation of size that is consistent with the disruption of the dPSS domains and a reorganization of the PEDOT crystals with the addition of DMSO, as illustrated in Figure 4b. This trend reverses with the addition of more DMSO (3%). However, the major radius remains

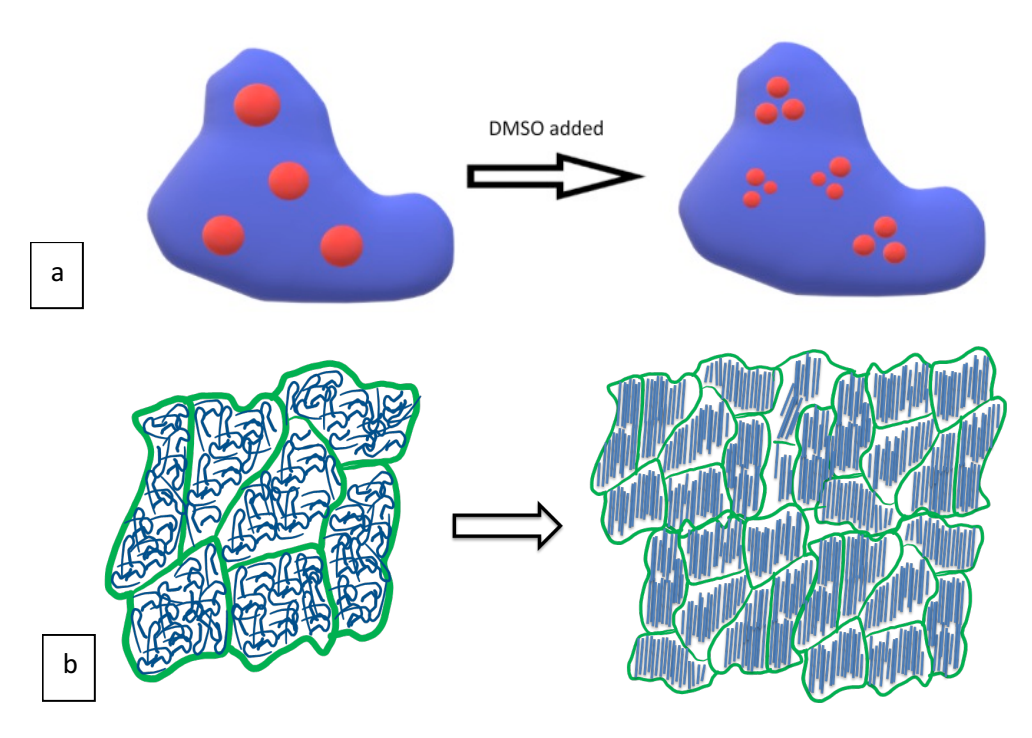


Figure 4 – Sketch to illustrate change in domain (a) and fibril structure (b) with the addition of DMSO to the pre-deposition aqueous solution of PEDOT:dPSS. Large dPSS domains with randomly oriented fibrils break-up and shrink when DMSO is added and PEDOT fibrils become well-aligned.

significantly greater than the minor radius, indicating that eccentric crystal domains are formed. The further addition of DMSO (5%) again reverses the size trends, where the elliptical cross section of the fibrils becomes more symmetric, shown by the decrease in r_{maj} and r_{min} . This variation indicates that the increase in DMSO to 5% drives the domains and PEDOT fibrils to eventually form a uniform elliptical shape.

This analysis indicates that the addition of DMSO initiates a reorganization of the fibrils that increases their packing and concurrently decreases the domain size. When PEDOT:dPSS is added to water, the hydrophilic dPSS domains encapsulate the hydrophobic PEDOT fibrils.

Furthermore, when the water evaporates during film formation, the dPSS domains trap the PEDOT fibrils in place. The observed changes in PEDOT radius and uniformity, combined with

the decrease in correlation length, show a decrease in all structure sizes from the micron to the nanoscale by nearly an order of magnitude with the addition of DMSO. Structural changes of this magnitude are consistent with the size and smoothness changes as well as conductivity increases reported by other groups. 9,10,12

Impact of Deposition Technique on Blend Structure

To monitor the impact of deposition procedure on the morphology and structure of the phase separated blend film, the neutron scattering curves of PEDOT:dPSS films formed by spray coating were also measured and analyzed as shown in Figure 2. A qualitative inspection of these curves shows similar trends to those observed in the films formed by spin coating, most notably as the decrease in low Q scattering of the PEDOT:dPSS blends with the addition of DMSO. Quantitatively, the decrease in domain size (as monitored by the correlation length) is consistent with that of the spin coated films. Spray coated films show a 70% decrease in domain size relative to those formed from the aqueous solution (10 microns to 2.9 microns) with the addition of 1% DMSO, followed by further decreases in domain size with additional DMSO (a 77% size reduction with 3% DMSO and 85% size reduction with 5% DMSO). As with the spin coated samples, the phase separated structure decreases systematically from that of the pure (0% DMSO) PEDOT:dPSS solutions. Given that the qualitative and quantitative changes in dPSS domain size in the film with addition of DMSO to the pre-deposition solution is very similar for both deposition techniques, it appears that the morphological changes in the film are due to the structural changes of the blend in the pre-deposition solution with addition of DMSO and not a result of the mechanics of the film formation processes associated with the deposition technique.

Analysis of the neutron scattering curves at smaller length scales (higher Q value) also shows similar morphological changes of the samples fabricated by the two deposition techniques. The addition of DMSO to the pre-deposition solution also results in PEDOT fibrillar domains that fluctuate in size with DMSO loading for the samples fabricated by spray coating. In the spray coated samples, the r_{min} initially decreases with added DMSO, followed by an increase in domain size at 3% DMSO and a slight decrease with 5% DMSO. The r_{mai} initially increases significantly with addition of 1% and 3% DMSO, then decreases as 5% DMSO is added to the pre-deposition solution, leading to a more symmetric cross-section of the PEDOT crystalline fibrils at this highest DMSO loading. These results, therefore, demonstrate the disruption of the PSS and PEDOT domains with DMSO addition to the pre-deposition solution is dominant in determining the structure of the PEDOT:dPSS phase separated polymer blend film. This is accompanied by a reorganization of the PEDOT fibrils with addition of DMSO. As the amount of DMSO is increased in the pre-deposition solution, the dPSS domains continue to break up into smaller domains, while the PEDOT fibrils become more uniformly aligned. This observation is consistent with an increase in packing density of the PEDOT fibrils within the smaller dPSS domains. Therefore, it appears that very similar morphological formation processes occur during film development in the spray coated films as with the spin-coated films.

Discussion

Figure 5 plots the domain size of the spin and spray coated samples as a function of amount of DMSO in the pre-deposition solution. Careful inspection shows that not only are the trends of the two samples similar, but quantitatively follow each other. This is exemplified by plotting the

ratio of the domain size in the spin coated samples to that in the spray coated samples, where this ratio is consistently about 50%. Thus, the domains in the spray-coated films are systematically twice as large as those in the spin-coated films. This observed difference in structure with a change in film formation conditions is consistent with reported smoothness and size changes showing that spin coated films have consistently smoother surfaces with increased conductivity relative to spray coated films. 10,12 This is also qualitatively consistent with the significant increase of conductivity of PSS:PEDOT films when 1% DMSO is added to the pre-deposition solution, which is followed by smaller increases in conductivity when increasing the DMSO concentration to 3% and 5%. 12

Given the similarity of the morphology of both the spin coated and spray coated films with the addition of DMSO, it is our interpretation that the structure of the deposited films are guided by the structure of the PSS:PEDOT assemblies that exist in solution prior to deposition. PSS:PEDOT forms aggregates in the aqueous solution. Consequently, addition of DMSO to a PEDOT:PSS aqueous solution disrupts the conductive PEDOT assemblies, thereby creating smaller PSS domains in solution, as depicted in Figure 4a. Even though the PEDOT fibrils remain encapsulated by a layer of PSS, the smaller fibril assemblies remain in proximity to one another and the distance between the domains decreases. The PSS layer between the fibril assemblies also decreases as a result. This thin insulating PSS layer with small PEDOT fibrils enables a relatively smooth and more conductive film to form which translates to the observed morphology of the domains in the film upon deposition. Thus, we ascribe the large increase in conductivity with the addition of up to 5% DMSO in the pre-deposition solution to the formation of smaller dPSS domains in solution with well aligned PEDOT fibrils.

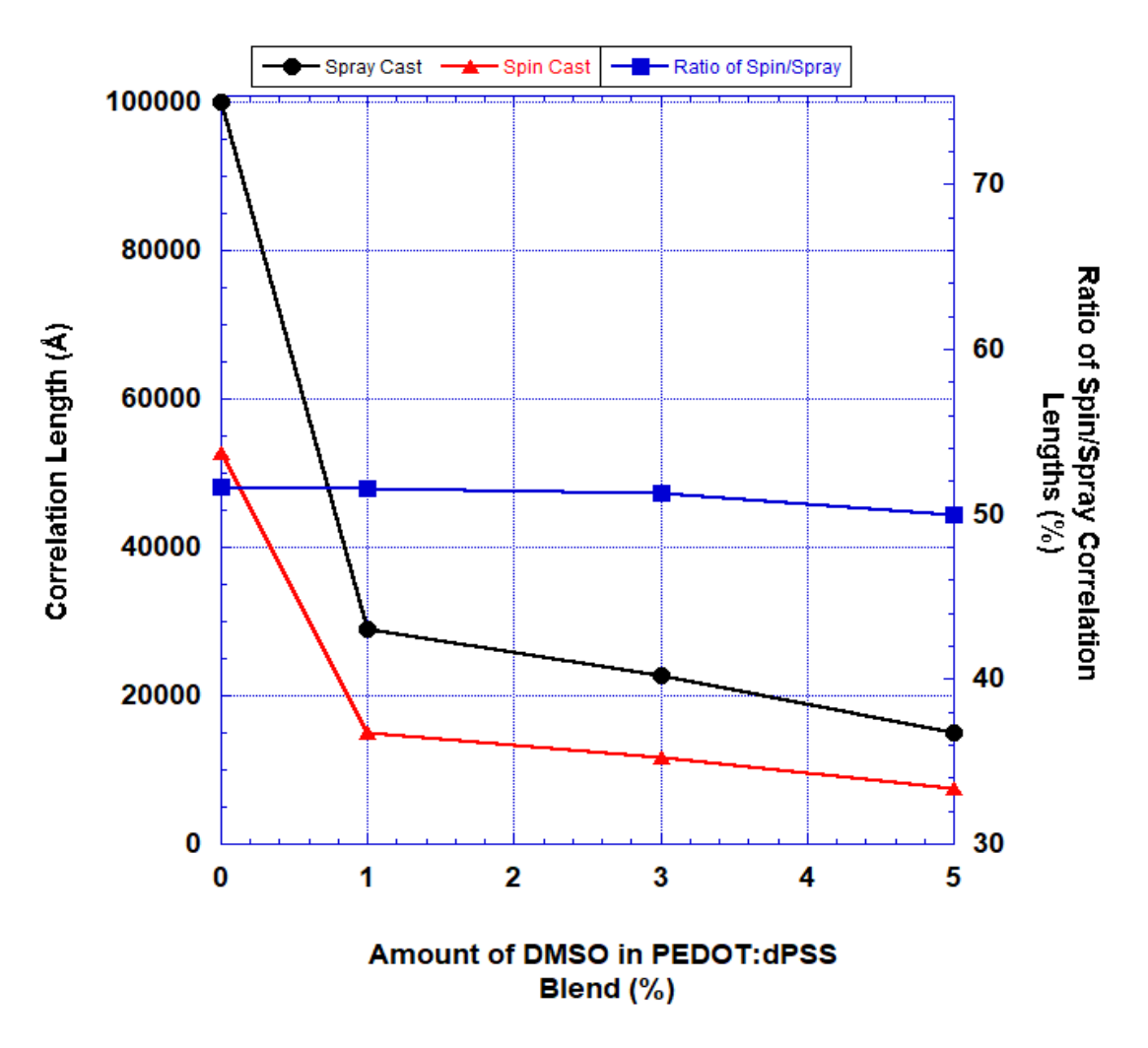


Figure 5 – Comparison of changes in domain size, as monitored by correlation length, of PSS:PEDOT films with the addition of DMSO to pre-deposition solutions for both spin (red triangles) and spray (black spheres) coated samples. The ratio of the correlation lengths of spin coated to spray coated films (blue squares) remains constant and is denoted on the right axis.

However, the difference in domain size in the phase separated blend films with coating procedure appears to be primarily influenced by solvent evaporation during film formation. The formation of consistently smaller domains in the films deposited using spin coating are attributed to the faster evaporation times commonly experienced in spin-coating techniques. For instance, in spin coating, the solution spreads quickly and evenly, coating the entire surface

while excess solvent in the solution is cast beyond the edge of the Si substrate. Subsequent drying allows the remaining solvent to evaporate quickly and evenly throughout the film. In comparison, when spray coating a solution onto a silicon substrate, the small droplets of solution impact the surface and dynamically spread in a localized area, each leaving a polymer solution droplet on the film surface. Additional spray passes deposit additional droplets. By dynamically wetting the substrate, a uniform film is created on the surface. During film formation, the solvent coalesces as a thicker layer on top of the film than that in the spin coated samples. Evaporation time of the solvent during annealing takes longer in spray coated samples than in spin-coated, and this slow drying allows for the polymer to aggregate more in the process. Smaller domains are therefore found in the faster evaporating spin coated samples than in the spray coated samples. Thus, samples formed by spin-coating exhibit a more well dispersed network of smaller connected domains than spray coated samples, which results in smoother surfaces and improved performance. It is interesting that this variation with coating technique does not fluctuate with the addition of DMSO to the solution, strongly suggesting that the presence of the DMSO does not alter the relative evaporation kinetics of the two deposition techniques.

A subset of the samples reported here (pristine and 5%wt DMSO PEDOT:dPSS films created by spray coating) coincide with samples that have previously been studied using SANS/USANS.¹⁰ Qualitatively, the results reported here are consistent with those reported previously, however previous studies report smaller domain and PEDOT fibrillar structures. We believe that the quantitative differences are due to variations in substrate and slight deviation in deposition conditions that were required to enable the direct comparison of spin and spray

coated samples in this study. These changes resulted in the formation of thicker samples in this study than were examined on the previous study. The thicker films contain larger domains and aggregates, as demonstrated by the large correlation lengths reported in Table 1. It is interesting that the impact of this increased film thickness does not appear to alter the underlying physics that control film formation with the addition of DMSO to the pre-deposition solution, as the structure of dPSS domains and PEDOT fibrils in the final conjugated polymer blend film follow similar trends for all systems studied.

Conclusions

The neutron scattering results reported here provide insight into the structure of PEDOT:dPSS thin films over length scales that range from angstroms to microns. These results show that the addition of DMSO to pre-deposition PEDOT:dPSS polymer blend aqueous solutions significantly decreases the correlation length of the fabricated phase separated blend film, regardless of deposition technique. The decrease in correlation length is greatest when just 1% DMSO is added to the PEDOT:dPSS polymer blend and continues to decrease with the addition of 3% DMSO and 5% DMSO. These results demonstrate an increased dispersion of the PSS domains, which results in the improved alignment of PEDOT fibrils within the domains. Smaller domains with well aligned fibrils are consistent with previously observed increased conductivity of PEDOT:PSS films formed from solutions containing DMSO.

Spin coating PEDOT:dPSS films resulted in consistently smaller domains than ultra-sonic spray coating due to faster evaporation times, which inhibits aggregation of domains and traps the aligned PEDOT fibrils. However, the qualitative similarity in the changes in blend

morphology for films formed with the two deposition techniques is interpreted to indicate that the structures of the deposited films are intimately dependent on the structure of the PSS:PEDOT assemblies that exist in solution prior to deposition. These results therefore provide important structural insight into the film formation process in conjugated polymer blend films, which is valuable in rationally designing film fabrication procedures to attain targeted morphologies and performance.

Acknowledgement

This work was supported by the National Science Foundation DMR-1808946. A portion of this research used resources at the High Flux Isotope Reactor and Spallation Neutron Source, a DOE Office of Science User Facility operated by the Oak Ridge National Laboratory. Access to CHRNS Very Small Angle Neutron Scattering provided by the Center for High Resolution Neutron Scattering, a partnership between the National Institute of Standards and Technology and the National Science Foundation under Agreement No. DMR-2010792. We acknowledge the support of the National Institute of Standards and Technology, U.S. Department of Commerce, in providing the neutron research facilities used in this work.

References

- Heuer, H. W.; Wehrmann, R.; Kirchmeyer, S. Electrochromic window based on conducting poly (3,4-ethylenedioxythiophene)poly(styrene sulfonate). Advanced Functional Materials 2002, 12 (2), 89-94 DOI: 10.1002/1616-3028(20020201)12:2<89::aid-adfm89>3.0.co;2-1.
- Andersson, P.; Nilsson, D.; Svensson, P. O.; Chen, M. X.; Malmstrom, A.; Remonen,
 T.; Kugler, T.; Berggren, M. Active matrix displays based on all-organic
 electrochemical smart pixels printed on paper. Advanced Materials 2002, 14 (20),
 1460-+ DOI: 10.1002/1521-4095(20021016)14:20<1460::aid-adma1460>3.0.co;2-s.
- Daoud, W. A.; Xin, J. H.; Szeto, Y. S. Polyethylenedioxythiophene coatings for humidity, temperature and strain sensing polyamide fibers. Sensors and Actuators B-Chemical 2005, 109 (2), 329-333 DOI: 10.1016/j.snb.2004.12.067.
- Poudel, B.; Hao, Q.; Ma, Y.; Lan, Y.; Minnich, A.; Yu, B.; Yan, X.; Wang, D.; Muto, A.;
 Vashaee, D.; Chen, X.; Liu, J.; Dresselhaus, M.; Chen, G.; Ren, Z. High-Thermoelectric
 Performance of Nanostructured Bismuth Antimony Telluride Bulk Alloys, Science,
 2008, 320 (5876), 634-638 DOI:10.1126/science.1156446
- Venkatasubramanian, R.; Siivola, E.; Colpitts, T.; O'Quinn, B. Thin-film thermoelectric devices with high room-temperature figures of merit, Nature, 2001, 413 (6856) 597-602 DOI: 10.1038/35098012
- Xia, Y. J.; Sun, K.; Ouyang, J. Y. Solution-Processed Metallic Conducting Polymer Films as Transparent Electrode of Optoelectronic Devices. Advanced Materials 2012, 24 (18), 2436-2440 DOI: 10.1002/adma.201104795.

- Bubnova, O.; Khan, Z.U.; Malti, A.; Braun, S.; Fahlman, M.; Berggren, M.; Crispin, X.
 Optimization of the thermoelectric figure of merit in the conducting polymer poly(3,4-ethylenedioxythiophene). Nature Materials 2011, 10 (6), 429-433 DOI: 10.1038/NMAT3012
- Kim, G. H.; Shao, L.; Zhang, K.; Pipe, K. P. Engineered doping of organic semiconductors for enhanced thermoelectric efficiency. Nature Materials 2013, 12 (8), 719-723 DOI: 10.1038/nmat3635.
- Dimitriev, O. P.; Grinko, D. A.; Noskov, Y. V.; Ogurtsov, N. A.; Pud, A. A. PEDOT:PSS films-Effect of organic solvent additives and annealing on the film conductivity.
 Synthetic Metals 2009, 159 (21-22), 2237-2239 DOI:
 10.1016/j.synthmet.2009.08.022.
- 10. Etampawala, T.; Tehrani, M.; Nematollahi, A.; He, L. L.; Dadmun, M. The impact of solvent doping on the morphology and performance of spray-coated PEDOT:dPSS: A USANS and SANS study. Organic Electronics 2017, 51, 86-93 DOI: 10.1016/j.orgel.2017.08.030.
- 11. Murphy, R. J.; Weigandt, K. M.; Uhrig, D.; Alsayed, A.; Badre, C.; Hough, L.; Muthukumar, M. Scattering Studies on Poly(3,4-ethylenedioxythiophene)-Polystyrenesulfonate in the Presence of Ionic Liquids. Macromolecules 2015, 48 (24), 8989-8997 DOI: 10.1021/acs.macromol.5b02320.
- 12. Zabihi, F.; Xie, Y.; Gao, S.; Eslamian, M. Morphology, conductivity, and wetting characteristics of PEDOT:PSS thin films deposited by spin and spray coating. Applied Surface Science 2015, 338, 163-177 DOI: 10.1016/j.apsusc.2015.02.128.

- 13. Kim, J. Y.; Jung, J. H.; Lee, D. E.; Joo, J. Enhancement of electrical conductivity of poly(3,4-ethylenedioxythiophene)/poly(4-styrenesulfonate) by a change of solvents. Synthetic Metals 2002, 126 (2-3), 311-316 DOI: 10.1016/s0379-6779(01)00576-8.
- 14. Ouyang, J.; Xu, Q. F.; Chu, C. W.; Yang, Y.; Li, G.; Shinar, J. On the mechanism of conductivity enhancement in poly (3,4-ethylenedioxythiophene): poly(styrene sulfonate) film through solvent treatment. Polymer 2004, 45 (25), 8443-8450 DOI: 10.1016/j.polymer.2004.10.001.
- 15. Kim, Y. H.; Sachse, C.; Machala, M. L.; May, C.; Muller-Meskamp, L.; Leo, K. Highly Conductive PEDOT:PSS Electrode with Optimized Solvent and Thermal Post-Treatment for ITO-Free Organic Solar Cells. Advanced Functional Materials 2011, 21 (6), 1076-1081 DOI: 10.1002/adfm.201002290.
- 16. Ashizawa, S.; Horikawa, R.; Okuzaki, H. Effects of solvent on carrier transport in poly(3,4-ethylenedioxythiophene)/poly(4-styrenesulfonate). Synthetic Metals 2005, 153 (1-3), 5-8 DOI: 10.1016/j.synthmet.2005.07.214.
- 17. Heller, W. T.; Cuneo, M.; Debeer-Schmitt, L.; Do, C.; He, L. L.; Heroux, L.; Littrell, K.; Pingali, S. V.; Qian, S.; Stanley, C.; Urban, V. S.; Wu, B.; Bras, W. The suite of small-angle neutron scattering instruments at Oak Ridge National Laboratory. Journal of Applied Crystallography 2018, 51, 242-248 DOI: 10.1107/s1600576718001231.
- 18. Groenendaal, B. L.; Jonas, F.; Freitag, D.; Pielartzik, H.; Reynolds, J. R. Poly(3,4-ethylenedioxythiophene) and its derivatives: Past, present, and future. Advanced Materials 2000, 12 (7), 481-494.

- 19. Jonas, F.; Heywang, G. TECHNICAL APPLICATIONS FOR CONDUCTIVE POLYMERS.

 Electrochimica Acta 1994, 39 (8-9), 1345-1347 DOI: 10.1016/0013-4686(94)e0057-7.
- 20. Jonas, F.; Krafft, W.; Muys, B. POLY(3,4-ETHYLENEDIOXYTHIOPHENE) CONDUCTIVE COATINGS, TECHNICAL APPLICATIONS AND PROPERTIES. Macromolecular Symposia 1995, 100, 169-173 DOI: 10.1002/masy.19951000128.
- 21. Jukes, P. C.; Martin, S. J.; Higgins, A. M.; Geoghegan, M.; Jones, R. A. L.; Langridge, S.; Wehrum, A.; Kirchmeyer, S. Controlling the surface composition of poly(3,4-ethylene dioxythiophene)poly(styrene sulfonate) blends by heat treatment. Advanced Materials 2004, 16 (9-10), 807-+ DOI: 10.1002/adma.200306487.
- 22. Lefebvre, M.; Qi, Z. G.; Rana, D.; Pickup, P. G. Chemical synthesis, characterization, and electrochemical studies of poly(3,4-ethylenedioxythiophene)/poly(styrene-4-sulfonate) composites. Chemistry of Materials 1999, 11 (2), 262-268 DOI: 10.1021/cm9804618.
- 23. Wignall, G. D.; Bates, F. S. ABSOLUTE CALIBRATION OF SMALL-ANGLE NEUTRON-SCATTERING DATA. Journal of Applied Crystallography 1987, 20, 28-40 DOI: 10.1107/s0021889887087181.
- 24. Wignall, G. D.; Littrell, K. C.; Heller, W. T.; Melnichenko, Y. B.; Bailey, K. M.; Lynn, G. W.; Myles, D. A.; Urban, V. S.; Buchanan, M. V.; Selby, D. L.; Butler, P. D. The 40 m general purpose small-angle neutron scattering instrument at Oak Ridge National Laboratory. Journal of Applied Crystallography 2012, 45, 990-998 DOI: 10.1107/s0021889812027057.

- 25. Barker, J. G.; Glinka, C. J.; Moyer, J. J.; Kim, M. H.; Drews, A. R.; Agamalian, M. Design and performance of a thermal-neutron double-crystal diffractometer for USANS at NIST. Journal of Applied Crystallography 2005, 38, 1004-1011 DOI: 10.1107/s0021889805032103.
- 26. Borreguero, J. M.; Campbell, S. I.; Delaire, O. A.; Doucet, M.; Goswami, M.; Hagen, M. E.; Lynch, V. E.; Proffen, T. E.; Ren, S.; Savici, A. T.; Sumpter, B. G.; Tms, Integrating Advanced Materials Simulation Techniques into an Automated Data Analysis Workflow at the Spallation Neutron Source. 2014; p 297-308.
- Kline, S.R.; Reduction and analysis of SANS and USANS data using IGOR ProJ. Appl.
 Cryst. 2006, 39, 895-900 https://doi.org/10.1107/S0021889806035059
- 28. Ilavsky, J. and P. R. Jemian (2009). "Irena: tool suite for modeling and analysis of small-angle scattering." Journal of Applied Crystallography 42: 347-353.
- 29. Archibald, R. K.; Doucet, M.; Johnston, T.; Young, S. R.; Yang, E.; Heller, W. T. Classifying and analyzing small-angle scattering data using weighted k nearest neighbors machine learning techniques. Journal of Applied Crystallography 2020, 53, 326-334 DOI: 10.1107/s1600576720000552.
- 30. Debye, P.; Bueche, A. M. SCATTERING BY AN INHOMOGENEOUS SOLID. Journal of Applied Physics 1949, 20 (6), 518-525 DOI: 10.1063/1.1698419.
- 31. Debye, P.; Anderson, H. R.; Brumberger, H. SCATTERING BY AN INHOMOGENEOUS SOLID .2. THE CORRELATION FUNCTION AND ITS APPLICATION. Journal of Applied Physics 1957, 28 (6), 679-683 DOI: 10.1063/1.1722830.

- 32. Svergun, D. I.; Semenyuk, A. V. SOLUTION OF INTEGRAL-EQUATIONS OF THE CONVOLUTION TYPE IN THE PROCESSING OF DATA ON SMALL-ANGLE EXPERIMENT.

 Kristallografiya 1987, 32 (6), 1365-1372.
- 33. Feigin, L.A.; Svergun, D.I. Structure Analysis by Small-Angle X-Ray and Neutron Scattering, Plenum, New York, (1987)
- 34. Newbloom, G.M; Weigandt, K.M.; Pozzo, D.C. Electrical, mechanical, and structural characterization of self-assembly in poly(3-hexylthiophene) organogel networks, Macromolecules 45 (2012) 3452-3462.
- 35. Chen, H.P.; Chen, J.H.; Yin, W.; Yu, X.; Shao, M.; Xiao, K.; Hong, K.L.; Pickel, D.L.; Kochemba, W.M.; Kilbey, S.M.; Dadmun, M.D. Correlation of polymeric compatibilizer structure to its impact on the morphology and function of P3HT: PCBM bulk heterojunctions, J. Mater. Chem. A 1 (2013) 5309e5319.

For Table of Contents only

